The combination of CD49b and CD229 reveals a subset of multipotent cells with short-term activity within the hematopoietic stem cell compartment

Ece Somuncular,[a] Tsu-Yi Su,[a] Özge Dumral,[a] Anne-Sofie Johansson,[a] Sidinh Luc[a,b]

[a]*Center for Hematology and Regenerative Medicine, Department of Medicine Huddinge, Karolinska Institutet, Stockholm, Sweden*

[b]*Hematology Center, Karolinska University Hospital, Stockholm, Sweden*

Correspondence: Sidinh Luc, PhD, Center for Hematology and Regenerative Medicine, Department of Medicine Huddinge, Karolinska Institutet, Medicinaren 25/Neo, 14183 Huddinge, Sweden; E-mail: Sidinh.Luc@ki.se

RUNNING TITLE: CD49b and CD229 identify MPPs in the HSC pool

KEYWORDS: Hematopoiesis, hematopoietic stem cells, multipotent progenitors, blood cells, CD49b

AUTHOR CONTRIBUTIONS

E.S: collection and/or assembly of data, data analysis and interpretation, study planning, manuscript writing.

T-Y.S: collection and/or assembly of data, data analysis and interpretation, manuscript writing.

Ö.D: collection and/or assembly of data.

A-S.J: collection and/or assembly of data, provision of study material, study planning, supervision.

S.L: conception and design, data analysis and interpretation, study planning, manuscript writing, financial support, supervision.

All authors discussed the result and approved the manuscript before submission.

ABSTRACT

Hematopoiesis is maintained by hematopoietic stem cells (HSCs) that replenish the blood lineages throughout life. It is well-established that the HSC pool is functionally heterogeneous consisting of cells differing in longevity, self-renewal ability, cell proliferation, and lineage differentiation. Although HSCs can be identified through the $Lin^{-}Sca\text{-}1^{+}c\text{-}Kit^{+}CD48^{-}CD34^{-}CD150^{+}$ immunophenotype, the cell surface marker combination does not permit the absolute purification of functional HSCs with long-term (LT) reconstituting ability. Prospective isolation of LT HSCs is crucial for mechanistic understanding of the biological functions of HSCs, and for resolving the functional heterogeneity within the HSC population. Here, we show that the combination of CD229 and CD49b cell surface markers within the phenotypic HSC compartment identifies a subset of multipotent progenitor cells with high proliferative activity and short-term reconstituting ability. Thus, functional HSCs can be prospectively isolated by the addition of CD229 and CD49b to conventional HSC markers.

SIGNIFICANCE STATEMENT

Blood cells are generated by rare stem cells throughout life. Based on their defining features of self-renewal and multipotent abilities, blood stem cells are used in transplantation as curative treatment for blood diseases. Despite their clinical importance, the mechanisms of stem cell properties are elusive given the inability to isolate pure blood stem cells and prospective assessment of their functions. In this study, we demonstrate that functional stem cells can be isolated by using the cell surface markers CD229 and CD49b. Our study has important implications for the analysis of mechanisms regulating stem cell function and is of relevance for clinical applications of stem cells.

INTRODUCTION

The hematopoietic system is composed of short-lived mature blood cells and multipotent progenitors that are replenished by infrequent hematopoietic stem cells (HSCs). The hallmarks of HSCs are multipotency and the ability of self-renewal [1,2]. Although HSCs can be separated from differentiated cells by immunophenotype, HSCs can only be distinguished from multipotent progenitors (MPPs) with limited or short-term (ST) self-renewal potential through functional studies. Hematopoietic stem cell function is experimentally defined by the ability to continuously repopulate mature blood lineages in myeloablated mice for at least 4-6 months, and the capacity to reconstitute secondary transplanted animals [2]. Through *in vivo* limiting dilution and clonal studies, the HSC population was demonstrated to be heterogeneous in self-renewal ability, longevity, repopulation efficiency, and lineage differentiation output [3–10]. The mechanistic basis for the distinct behavior of HSCs is not well elucidated, however, epigenetic mechanisms have been suggested to play a role [11,12].

Hematopoietic stem cells reside within the phenotypically defined Lin^{-}Sca-1^{+}c-Kit^{+} (LSK) compartment and can be further enriched through CD34^{-} [13], Flt-3^{-} [14], CD48^{-}, and CD150^{+} [15] cell surface marker selections. The additional inclusion of CD49b [11] or CD229 [16] have been suggested to resolve functionally distinct subsets of HSCs. However, a significant proportion of the cells still lack long-term (LT) reconstituting ability. Therefore, prospective identification of functional HSCs remains crucial to resolve the heterogeneity and to permit mechanistic analysis of distinct HSC behavior. Here, we used a combination of CD49b and CD229 to subfractionate the conventional phenotypic HSC compartment. We identified a CD49b^{+}CD229^{+} subset of MPPs with high proliferative activity and short-term reconstituting ability. Our study demonstrates that inclusion of additional cell surface markers to the conventional HSC immunophenotype can improve the identification of functional HSCs.

MATERIALS AND METHODS

Animal experiments

All animal experiments were approved by the Swedish regional ethical committee, Linköping ethical committee (ethical number 882 and 02250-2022). Animals were bred at the Preclinical Laboratory at Karolinska University hospital. Female and male C57BL/6J mice, 8-17 weeks old, were used. In transplantation experiments, the Gata-1 eGFP (CD45.2) [17] mouse strain, backcrossed onto a C57BL/6J background (>8 generations), was used as a donor strain and B6.SJL-PtprcaPepcb/BoyCrl and B6.SJL-PtprcaPepcb/BoyJ mice (CD45.1) were used as recipients. Recipients were lethally irradiated with 10 Gy split over two days. In primary transplantation, five donor cells (CD45.2), along with 200,000 bone marrow (BM) support cells (CD45.1), were transplanted via tail vein injection. In secondary transplantation, 10 million unfractionated BM cells from primary transplanted recipients were intravenously injected into 1-2 lethally irradiated mice per primary donor mouse.

The threshold for successfully repopulated mice was based on ≥0.1% CD45.2 and/or eGFP^{+} platelet reconstitution in the peripheral blood (PB) two months post-transplantation. Repopulation of mature blood cells in the PB (platelets, erythrocytes, myeloid, B, T, and NK cells) was only considered if reconstitution was ≥0.01% and had ≥10 events in the CD45.2 donor gate for any given lineage. To determine the number of LT myeloid reconstituted mice, the threshold was set to ≥0.1% reconstitution in the PB for myeloid cells evaluated 6 months post-transplantation. Using the number of LT myeloid reconstituted mice, HSC frequencies was estimated by limiting dilution analysis through the online tool https://bioinf.wehi.edu.au/software/elda/, calculated with a 95% confidence interval [18].

Flow Cytometry experiments

Bone marrow and PB cells were prepared and stained with antibodies (Supporting Information Table S1), as previously described [11]**.** Cell cycle and cell proliferation analyses were performed according to manufacturer's protocols (BD Biosciences) and previous studies [11,19]. Cells were sorted using FACSAria™ Fusion (BD Biosciences) and analyzed on LSR Fortessa™ or FACSymphony™ A5 (BD Biosciences). Fluorescent minus one (FMO) controls were included in all experiments. Gates were set based on FMO controls, backgating, or negative cell populations. Purity analysis was performed in all cell sorting experiments with a mean purity of 88% (±9%). Post-acquisition analyses were performed on FlowJo software v10 (BD Biosciences).

In vitro Assays

Combined myeloid and B cell lineage differentiation potential of single sorted cells was assessed *in vitro* using the OP9 co-culture assay as previously described [20,21]. Cultures were evaluated by flow cytometry analysis three weeks post-sort.

Statistical Analysis

Statistical analyses were performed using GraphPad version 9.4.1 for Mac OS. Non-parametric analysis was performed with Kruskal Wallis test with Dunn's multiple comparison test or Mann-Whitney test. Data are represented as mean ± SD and *p*-values are shown.

RESULTS AND DISCUSSION

Hematopoietic stem cells reside within the phenotypic LSKCD48^{-}CD34^{-}CD150^{+} (CD150^{+}) compartment in the BM [2]. Several cell surface markers, including CD49b and CD229, have been suggested to further subfractionate the functionally heterogeneous CD150^{+} population into LT reconstituting HSCs with myeloid-bias (M-bi) or lymphoid-bias (L-bi), and MPPs with transient or limited self-renewal ability [11,16]. Here, we explored whether the combination of CD49b and CD229 can purify functionally defined HSCs, as well as HSCs with distinct behaviors. CD49b and CD229 subfractionation revealed four immunophenotypic subtypes within the phenotypic LSKCD48^{-}CD34^{-}CD150^{hi} compartment, containing the most primitive HSCs [8,22,23]: CD49b^{-}CD229^{-}, CD49b^{-}CD229^{+}, CD49b^{+}CD229^{-}, and CD49b^{+}CD229^{+} (Fig. 1A; Supporting Information Fig. S1A). We first analyzed the cell cycle status to investigate whether cycling differences could distinguish between the subtypes. All four fractions were predominantly found in the G0 phase of cell cycle; however, CD49b^{-}CD229^{-} and CD49b^{-}CD229^{+} were most quiescent, whereas significantly more CD49b^{+}CD229^{-} and CD49b^{+}CD229^{+} cells were found in the G1 phase (Fig. 1B, 1D). Consistent with the cell cycle data, BrdU incorporation analysis showed that CD49b^{+}CD229^{-} and CD49b^{+}CD229^{+} subsets were most proliferative among the four subsets (Fig. 1C, 1E). These findings suggest that CD49b^{-} subsets represent the most dormant cells, regardless of CD229 expression, consistent with previous data [11].

Given that CD49b and CD229 have both been described to enrich for cells with L-bi [11,16], we investigated the multilineage differentiation ability of CD49b^{-}CD229^{-}, CD49b^{-}CD229^{+}, CD49b^{+}CD229^{-}, and CD49b^{+}CD229^{+} cells. All four populations were competent in clonally generating B lymphocytes and myeloid cells *in vitro* (Fig. 1F; Supporting Information Fig. S1B). To assess the multilineage ability *in vivo*, we performed competitive transplantation using limiting numbers of each subtype (five cells per animal). The success rate of transplantation ranged between 73-86% (CD49b^{-}CD229^{-}, 81%; CD49b^{-}CD229^{+}, 86%;

CD49b$^+$CD229$^-$, 73%; and CD49b$^+$CD229$^+$, 81%). The comparable transplantation efficiency between the subsets suggest that the subtypes have similar homing ability. All four populations also exhibited similar efficiency in total blood leukocyte repopulation over the course of six months, and were capable of multilineage differentiation (Fig. 2A, 2B). Notably, the CD49b$^+$CD229$^+$ subtype was the only population with declining myeloid, platelet, and erythrocyte reconstitution with time, while other subsets had either increasing, or stable LT repopulation of all blood lineages (Fig. 2B; Supporting Information Fig. S1C, S1D). This finding indicates that CD49b$^+$CD229$^+$ cells have reduced reconstituting ability and limited self-renewal potential. Indeed, only 46% of the CD49b$^+$CD229$^+$ transplanted mice were able to actively produce short-lived myeloid cells six months after transplantation (Fig. 2C). Additionally, CD49b$^+$CD229$^+$ transplanted mice exhibited a stronger preference for lymphoid cells in the PB, consistent with the reduced myeloid output (Fig. 2D). In further agreement, the CD49b$^+$CD229$^+$ subtype generated myeloid cells with the lowest efficiency among the four populations, but potently gave rise to lymphoid cells in the BM (Fig. 2E). In contrast, CD49b$^-$CD229$^-$, CD49b$^-$CD229$^+$, and CD49b$^+$CD229$^-$ subtypes demonstrated robust myeloid reconstitution in the PB and BM, suggesting high self-renewal potential (Fig. 2B-2E). Remarkably, the CD49b$^-$CD229$^+$ population also showed a stronger lymphoid differentiation profile in the PB, indicating that CD49b and CD229 subfractionation may distinguish between HSCs with distinct repopulation characteristics, in addition to differences in self-renewal potential (Fig. 2D; Supporting Information Fig. S2).

To further address the differences in reconstitution and self-renewal potential, we assessed the ability of CD49b$^-$CD229$^-$, CD49b$^-$CD229$^+$, CD49b$^+$CD229$^-$, and CD49b$^+$CD229$^+$ cells to regenerate the stem- and progenitor cells. Only 54% of the CD49b$^+$CD229$^+$ transplanted mice were capable of reconstituting phenotypic HSCs and the repopulation efficiency was additionally significantly lower in this group (Fig. 2F, 2G). These results are consistent with a reduced regenerative capacity in CD49b$^+$CD229$^+$ cells. In further agreement, the number of

CD49b$^+$CD229$^+$ transplanted mice capable of repopulating LMPP, CLP, GMP, and MkP progenitor cells was markedly reduced compared to other subtypes (Supporting Information Fig. S3). Collectively, these results suggest that the CD49b$^+$CD229$^+$ subset does not contain HSC activity, but rather represent MPPs with short-term repopulating capacity. Therefore, to estimate the frequency of functional HSCs in the CD49b$^-$CD229$^-$, CD49b$^-$CD229$^+$, CD49b$^+$CD229$^-$, and CD49b$^+$CD229$^+$ subsets, we made use of data from our limiting number transplantation to quantify stem cell frequency. Using limiting dilution calculation [18,24], the frequency of functional HSCs was predicted to be the lowest in the CD49b$^+$CD229$^+$ subset, in line with the lower reconstituting ability and lack of HSC activity (Fig. 2H).

To further investigate whether the self-renewal potential is indeed lower in the CD49b$^+$CD229$^+$ subset, we selected transplanted mice, which had reconstituted the HSC compartment (Fig. 2F, 2G), for secondary transplantation to assess their long-term reconstituting ability. Although the four populations were able to repopulate all secondary recipients, the CD49b$^+$CD229$^+$ subtype was the least efficient in repopulating blood leukocytes and had declining repopulation activity over time (Fig. 3A). The poor repopulating activity was observed in both myeloid and lymphoid lineages, consistent with CD49b$^+$CD229$^+$ cells lacking extensive self-renewal potential (Fig. 3B). We therefore assessed the number of animals exhibiting extensive LT myeloid reconstitution 6 months following secondary transplantation and observed that three out of four mice in the CD49b$^+$CD229$^+$ group had extensive myeloid repopulating activity (Fig. 3C). These data, in combination with the estimated stem cell frequency from primary transplantation (Fig. 2H), indicate that the actual stem cell frequency in the CD49b$^+$CD229$^+$ subset is likely even lower than the estimated frequency. Conversely, CD49b$^-$CD229$^-$ and CD49b$^-$CD229$^+$ subsets had the most potent reconstituting ability to all blood lineages, whereas CD49b$^+$CD229$^-$ was highly efficient in generating lymphoid cells (Fig. 3B). We have previously shown that CD49b$^+$ HSCs, without CD229 subfractionation, contain rare LT HSCs with lymphoid bias. Based on single cell transplantation the HSC frequency in

CD49b$^+$ HSCs is estimated to be 11% (9/79 myeloid reconstituted mice, 5-6 months post-transplantation) [11]. The preferential lymphoid repopulation over time in the CD49b$^+$CD229$^-$ subset suggests that lymphoid-biased HSCs residing within CD49b$^+$ LT HSCs can be enriched using the CD229 marker (Fig. 2H, 3B). Altogether, these findings demonstrate that the CD49b$^+$CD229$^+$ subset within the phenotypic HSC compartment predominantly represents MPPs with higher proliferative activity and ST reconstituting ability, and therefore do not represent functional HSCs. In contrast, LT HSCs are confined to the CD49b$^-$CD229$^-$, CD49b$^-$CD229$^+$ and CD49b$^+$CD229$^-$ subsets.

CONCLUSION

It is well-recognized that HSCs isolated by immunophenotype alone will contain cells lacking *in vivo* LT reconstituting ability. Therefore, assessment of stem cell function has been constricted to retrospective analysis through transplantation assays where HSCs are defined based on functional readout [2]. The inability to prospectively identify functional HSCs has limited the mechanistic insights into blood stem cell regulation, as molecular analysis of immunophenotypic HSCs does not reflect HSC specific function and behavior, but rather a composite of HSCs and MPPs with short-term reconstituting potential. Therefore, identifying strategies for prospective isolation of functional HSCs continues to be necessary to permit the study of regulatory mechanisms of HSC function, development, and differentiation. In this study, we evaluated whether the combination of CD49b and CD229 cell surface marker expression within the conventional phenotypic HSC compartment can resolve the functional heterogeneity and refine the identification of HSCs. We demonstrate that the transient and ST reconstituting activity of phenotypic HSCs is predominantly confined to the CD49b$^+$CD229$^+$ fraction, which contained the lowest HSC frequency and failed to maintain LT hematopoiesis. Furthermore, in a previous study, we identified a fraction of phenotypic HSCs expressing CD49b that are enriched for LT HSCs with lymphoid bias [11]. Our current findings indicate that through the segregation of

CD49b^{+}CD229^{+} cells, the lymphoid-biased LT HSCs can be further enriched in the CD49b^{+}CD229^{-} subset. Moreover, our results implicate that the combination of CD49b and CD229 likely differentiates HSCs with additional distinct behaviors. In conclusion, we demonstrate that functional HSCs with extensive self-renewal ability can be prospectively enriched by discriminating and excluding CD49b^{+}CD229^{+} MPPs with ST reconstituting activity. Our study provides the basis for prospective isolation of HSCs with improved purity and permits a more accurate analysis of the molecular mechanisms underlying HSC specific function and behavior.

ACKNOWLEDGEMENTS

The authors thank Prof. C. Nerlov (University of Oxford) for providing the Gata-1 eGFP mouse strain and Prof. SE. Jacobsen for helpful discussions. S.L was supported by a Wallenberg Academy Fellow award (2016.0131) and by the Swedish Childhood Cancer Fund (TJ2017-0074, PR2017-0047). T-Y.S was supported by the KI Doctoral Education grant. This work was funded by the European Hematology Association, the Swedish Cancer Society (CAN2017/583, 20 1062 PjF), the Swedish Research Council (2016-02331), the Strategic research area (SFO) in Stem cell and Regenerative Medicine, Åke Olsson foundation and Åke Wiberg foundation.

DISCLOSURE OF POTENTIAL CONFLICT OF INTEREST

The authors declare no conflict of interest.

REFERENCES

1 Orkin SH, Zon LI. Hematopoiesis: An Evolving Paradigm for Stem Cell Biology. Cell 2008;132:631–644.

2 Wilkinson AC, Igarashi KJ, Nakauchi H. Haematopoietic stem cell self-renewal in vivo and ex vivo. Nat Rev Genet 2020;21:541–554.

3 Carrelha J, Meng Y, Kettyle LM, et al. Hierarchically related lineage-restricted fates of multipotent haematopoietic stem cells. Nature 2018;554:106–111.

4 Sanjuan-Pla A, Macaulay IC, Jensen CT, et al. Platelet-biased stem cells reside at the apex of the haematopoietic stem-cell hierarchy. Nature 2013;502:232–236.

5 Yamamoto R, Morita Y, Ooehara J, et al. Clonal Analysis Unveils Self-Renewing Lineage-Restricted Progenitors Generated Directly from Hematopoietic Stem Cells. Cell 2013;154:1112–1126.

6 Yamamoto R, Wilkinson AC, Ooehara J, et al. Large-Scale Clonal Analysis Resolves Aging of the Mouse Hematopoietic Stem Cell Compartment. Cell Stem Cell 2018;22:600-607.e4.

7 Müller-Sieburg CE, Cho RH, Thoman M, et al. Deterministic regulation of hematopoietic stem cell self-renewal and differentiation. Blood 2002;100:1302–1309.

8 Morita Y, Ema H, Nakauchi H. Heterogeneity and hierarchy within the most primitive hematopoietic stem cell compartment. J Exp Med 2010;207:1173–1182.

9 Challen GA, Boles NC, Chambers SM, et al. Distinct Hematopoietic Stem Cell Subtypes Are Differentially Regulated by TGF-β1. Cell Stem Cell 2010;6:265–278.

10 Dykstra B, Kent D, Bowie M, et al. Long-Term Propagation of Distinct Hematopoietic Differentiation Programs In Vivo. Cell Stem Cell 2007;1:218–229.

11 Somuncular E, Hauenstein J, Khalkar P, et al. CD49b identifies functionally and epigenetically distinct subsets of lineage-biased hematopoietic stem cells. Stem Cell Rep 2022;17:1546–1560.

12 Haas S, Trumpp A, Milsom MD. Causes and Consequences of Hematopoietic Stem Cell Heterogeneity. Cell Stem Cell 2018;22:627–638.

13 Osawa M, Hanada K, Hamada H, et al. Long-term lymphohematopoietic reconstitution by a single CD34-low/negative hematopoietic stem cell. Science 1996;273:242–245.

14 Adolfsson J, Borge OJ, Bryder D, et al. Upregulation of Flt3 Expression within the Bone Marrow Lin−Sca1+c-kit+ Stem Cell Compartment Is Accompanied by Loss of Self-Renewal Capacity. Immunity 2001;15:659–669.

15 Kiel MJ, Yilmaz ÖH, Iwashita T, et al. SLAM Family Receptors Distinguish Hematopoietic Stem and Progenitor Cells and Reveal Endothelial Niches for Stem Cells. Cell 2005;121:1109–1121.

16 Oguro H, Ding L, Morrison SJ. SLAM Family Markers Resolve Functionally Distinct Subpopulations of Hematopoietic Stem Cells and Multipotent Progenitors. Cell Stem Cell 2013;13:102–116.

17 Drissen R, Buza-Vidas N, Woll P, et al. Distinct myeloid progenitor–differentiation pathways identified through single-cell RNA sequencing. Nat Immunol 2016;17:666–676.

18 Hu Y, Smyth GK. ELDA: Extreme limiting dilution analysis for comparing depleted and enriched populations in stem cell and other assays. J Immunol Methods 2009;347:70–78.

19 Luc S, Huang J, McEldoon JL, et al. Bcl11a Deficiency Leads to Hematopoietic Stem Cell Defects with an Aging-like Phenotype. Cell Reports 2016;16:3181–3194.

20 Nakano T, Kodama H, Honjo T. Generation of Lymphohematopoietic Cells from Embryonic Stem Cells in Culture. Science 1994;265:1098–1101.

21 Luc S, Luis TC, Boukarabila H, et al. The earliest thymic T cell progenitors sustain B cell and myeloid lineage potential. Nat Immunol 2012;13:412–419.

22 Kent DG, Copley MR, Benz C, et al. Prospective isolation and molecular characterization of hematopoietic stem cells with durable self-renewal potential. Blood 2009;113:6342–6350.

23 Beerman I, Bhattacharya D, Zandi S, et al. Functionally distinct hematopoietic stem cells modulate hematopoietic lineage potential during aging by a mechanism of clonal expansion. Proc National Acad Sci 2010;107:5465–5470.

24 Dykstra B, Olthof S, Schreuder J, et al. Clonal analysis reveals multiple functional defects of aged murine hematopoietic stem cells. J Exp Med 2011;208:2691–2703.

Figure 1. CD49b and CD229 are heterogeneously expressed in the phenotypic HSC compartment. **(A)**: Representative FACS profiles and gating strategy of the phenotypic HSC compartment (Lin^{-}Sca-1^{+}c-kit^{+} (LSK) CD48^{-}CD34^{-}CD150^{hi}) and further subfractionation with CD49b and CD229. **(B)**: Cell cycle analysis of CD49b^{-}CD229^{-}, CD49b^{-}CD229^{+}, CD49b^{+}CD229^{-}, and CD49b^{+}CD229^{+} subsets by Ki-67 and DAPI staining. Frequency of cells in G0 (left) and G1 (right) phases are shown. n = 9 biological replicates, 2 experiments. **(C):** Cell proliferation analysis by BrdU incorporation. Frequencies of BrdU^{+} CD49b^{-}CD229^{-}, CD49b^{-}CD229^{+}, CD49b^{+}CD229^{-}, and CD49b^{+}CD229^{+} cells are shown. n = 8 biological replicates, 2 experiments. **(D):** Representative FACS profile of cell cycle analysis. **(E)**: Representative FACS profile of BrdU proliferation analysis. **(F)**: *In vitro* analysis of the B cell and myeloid cell differentiation potential from single cell sorted CD49b^{-}CD229^{-}, CD49b^{-}CD229^{+}, CD49b^{+}CD229^{-}, and CD49b^{+}CD229^{+} populations using OP9 co-culture assay. Total frequencies of clones with B cells and/or B and myeloid cells (left), and clones containing only myeloid cells (right) are shown. n = 5 biological replicates, 2 experiments.

Data are represented as mean ± SD. Frequencies of parent gates are shown in FACS plots. Statistical analysis was performed using the Kruskal Wallis test with Dunn's multiple comparison test in (B-C, F). Abbreviations: FSC, forward scatter; SSC, side scatter; FSC-H, forward scatter height; FSC-A, forward scatter area; BrdU, Bromodeoxyuridine.

Figure 2. CD49b and CD229 subfractionate the phenotypic HSC compartment into functional HSCs and MPPs with short-term activity. **(A)**: Leukocyte repopulation in the peripheral blood of mice transplanted with 5 cells from CD49b^{-}CD229^{-}, CD49b^{-}CD229^{+}, CD49b^{+}CD229^{-}, and CD49b^{+}CD229^{+} populations. **(B)**: Donor-derived myeloid, platelet, erythrocyte, B cell, and T cell frequency in the PB of mice transplanted with 5 cells from CD49b^{-}CD229^{-}, CD49b^{-}CD229^{+}, CD49b^{+}CD229^{-}, and CD49b^{+}CD229^{+} populations. **(C)**: Proportion of transplanted mice with

≥0.1% donor-derived myeloid cells in the PB, 6 months post-transplantation. **(D)**: Relative myeloid and lymphoid (B, T, and natural killer cells) repopulation of reconstituted mice in the PB, 6 months post-transplantation. $n_{CD49b^-CD229^-}$ = 11, $n_{CD49b^-CD229^+}$ = 11, $n_{CD49b^+CD229^-}$ = 10, and $n_{CD49b^+CD229^+}$ = 9, 2 experiments. **(E)**: Relative donor-derived myeloid (M, left) and lymphoid (L, right) frequency (L: B, T, and natural killer cells) of reconstituted mice in the BM, 6 months post-transplantation. $n_{CD49b^-CD229^-}$ = 10, $n_{CD49b^-CD229^+}$ = 11, $n_{CD49b^+CD229^-}$ = 10, and $n_{CD49b^+CD229^+}$ = 9, 2 experiments. **(F)**: Donor-derived HSC ($Lin^-Sca\text{-}1^+c\text{-}kit^+Flt\text{-}3^-CD48^-CD150^+$) frequency in the BM of primary transplanted animals. $n_{CD49b^-CD229^-}$ = 11 mice, $n_{CD49b^-CD229^+}$ = 11 mice, $n_{CD49b^+CD229^-}$ = 10 mice, and $n_{CD49b^+CD229^+}$ = 7 mice, 2 experiments. **(G)**: Proportion of transplanted mice with phenotypic HSC reconstitution. **(H)**: Estimated HSC frequency based on limiting dilution calculation using the number of mice positively reconstituted in PB myeloid cells, 6 months post-transplantation.

$n_{CD49b^-CD229^-}$ = 13 mice, $n_{CD49b^-CD229^+}$ = 12 mice, $n_{CD49b^+CD229^-}$ = 11 mice, and $n_{CD49b^+CD229^+}$ = 13 mice, 2 experiments, in (A-C, G). Data are represented as mean ± SD in (A-B, D-F). Statistical analysis was performed using the Kruskal Wallis test with Dunn's multiple comparison test in (A-B and E-F) and the Mann-Whitney test in (D). Abbreviations: M, myeloid; L, lymphoid; HSC, hematopoietic stem cell

Figure 3. The $CD49b^+CD229^+$ subset lacks extensive long-term reconstituting ability. **(A)**: Leukocyte repopulation in the peripheral blood of secondary transplanted mice from $CD49b^-CD229^-$, $CD49b^-CD229^+$, $CD49b^+CD229^-$, and $CD49b^+CD229^+$ populations. **(B)**: Donor-derived myeloid, platelet, erythrocyte, B cell, and T cell frequency in the PB of secondary transplanted mice. $n_{CD49b^-CD229^-}$ = 9 mice, $n_{CD49b^-CD229^+}$ = 6-7 mice, $n_{CD49b^+CD229^-}$ = 5 mice, and $n_{CD49b^+CD229^+}$ = 4-5 mice, 1 experiment, in (A-B).

(C): Proportion of secondary transplanted mice with ≥0.1% donor-derived myeloid cells in the PB, 6 months post-transplantation. $n_{CD49b^{-}CD229^{-}}$ = 8 mice, $n_{CD49b^{-}CD229^{+}}$ = 6 mice, $n_{CD49b^{+}CD229^{-}}$ = 5 mice, and $n_{CD49b^{+}CD229^{+}}$ = 4 mice, 1 experiment.

Data are represented as mean ± SD in (A-B).

Figure 1

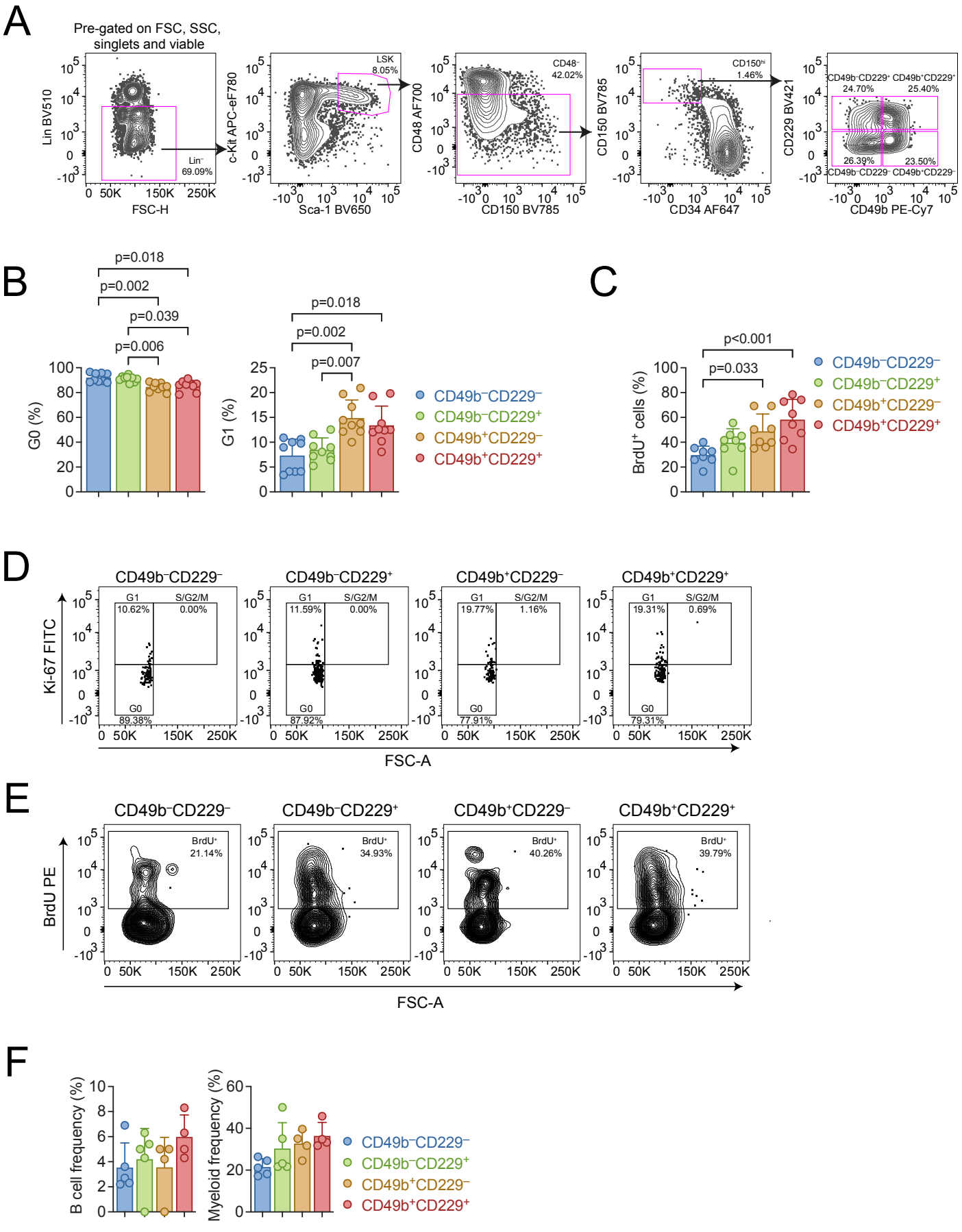
A
Pre-gated on FSC, SSC, singlets and viable
Lin BV510
FSC-H
Lin⁻ 69.09%
c-Kit APC-eF780
Sca-1 BV650
LSK 8.05%
CD48 AF700
CD150 BV785
CD48⁻ 42.02%
CD150 BV785
CD34 AF647
CD150ʰⁱ 1.46%
CD229 BV421
CD49b PE-Cy7
CD49b⁻CD229⁺ 24.70%
CD49b⁺CD229⁺ 25.40%
26.39%
23.50%
CD49b⁻CD229⁻
CD49b⁺CD229⁻
B
p=0.018
p=0.002
p=0.039
p=0.006
G0 (%)
p=0.018
p=0.002
p=0.007
G1 (%)
CD49b⁻CD229⁻
CD49b⁻CD229⁺
CD49b⁺CD229⁻
CD49b⁺CD229⁺
C
p<0.001
p=0.033
BrdU⁺ cells (%)
D
CD49b⁻CD229⁻
CD49b⁻CD229⁺
CD49b⁺CD229⁻
CD49b⁺CD229⁺
Ki-67 FITC
G1
S/G2/M
G0
10.62%
0.00%
89.38%
11.59%
0.00%
87.92%
19.77%
1.16%
77.91%
19.31%
0.69%
79.31%
FSC-A
E
BrdU PE
BrdU⁺ 21.14%
BrdU⁺ 34.93%
BrdU⁺ 40.26%
BrdU⁺ 39.79%
FSC-A
F
B cell frequency (%)
Myeloid frequency (%)
CD49b⁻CD229⁻
CD49b⁻CD229⁺
CD49b⁺CD229⁻
CD49b⁺CD229⁺

Figure 3

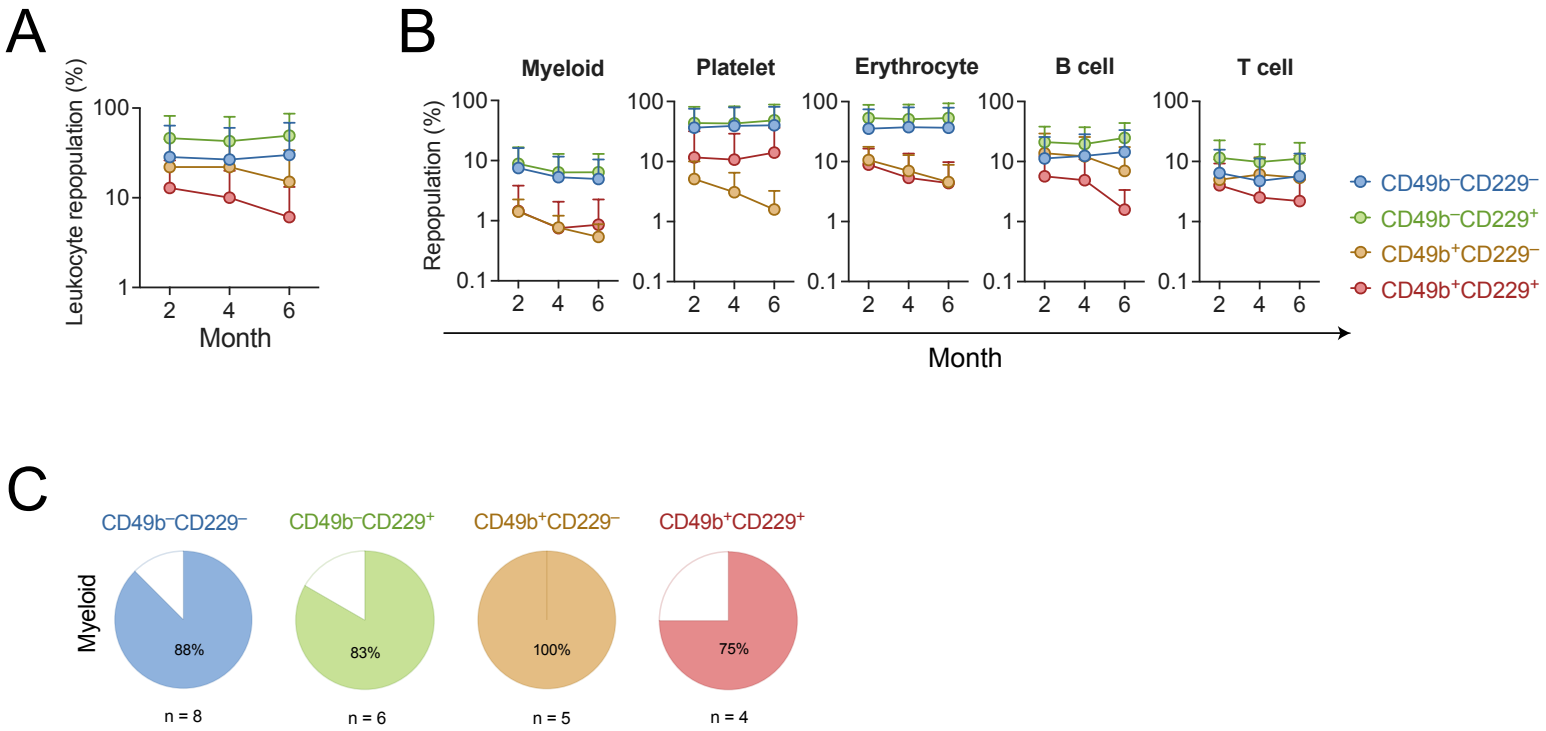
A
Leukocyte repopulation (%)
100
10
1
2
4
6
Month
B
Myeloid
Platelet
Erythrocyte
B cell
T cell
Repopulation (%)
100
10
1
0.1
2
4
6
Month
CD49b⁻CD229⁻
CD49b⁻CD229⁺
CD49b⁺CD229⁻
CD49b⁺CD229⁺
C
CD49b⁻CD229⁻
CD49b⁻CD229⁺
CD49b⁺CD229⁻
CD49b⁺CD229⁺
Myeloid
88%
83%
100%
75%
n = 8
n = 6
n = 5
n = 4

Figure 2

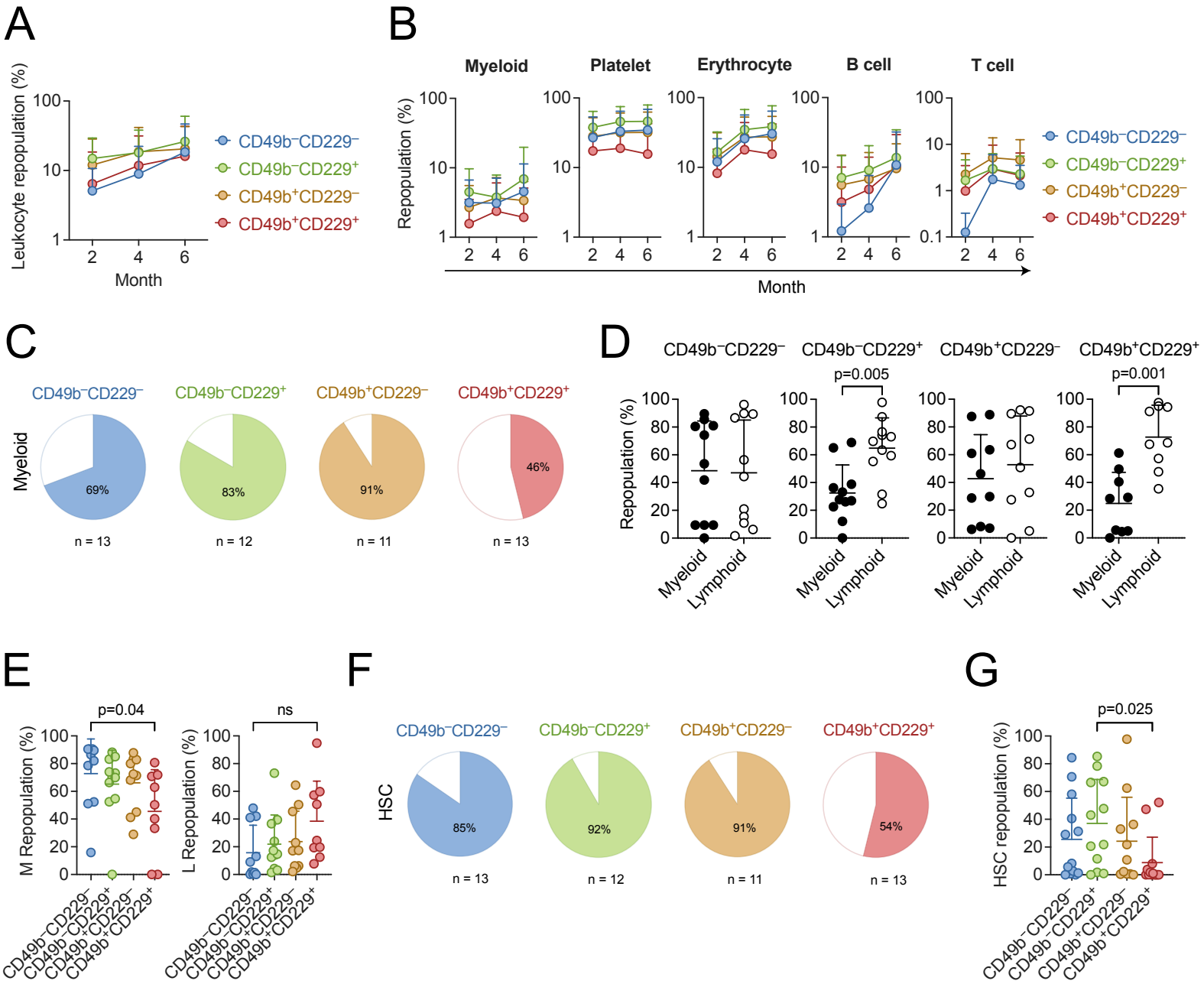

H

Subset	Estimated HSC frequency	
CD49b⁻CD229⁻	1/4.76	21%
CD49b⁻CD229⁺	1/3.32	30%
CD49b⁺CD229⁻	1/2.62	38%
CD49b⁺CD229⁺	1/8.59	12%